Photochemical & Photobiological Sciences

Accepted Manuscript

This is an *Accepted Manuscript*, which has been through the Royal Society of Chemistry peer review process and has been accepted for publication.

Accepted Manuscripts are published online shortly after acceptance, before technical editing, formatting and proof reading. Using this free service, authors can make their results available to the community, in citable form, before we publish the edited article. We will replace this *Accepted Manuscript* with the edited and formatted *Advance Article* as soon as it is available.

You can find more information about *Accepted Manuscripts* in the Information for Authors.

Please note that technical editing may introduce minor changes to the text and/or graphics, which may alter content. The journal's standard Terms & Conditions and the Ethical guidelines still apply. In no event shall the Royal Society of Chemistry be held responsible for any errors or omissions in this *Accepted Manuscript* or any consequences arising from the use of any information it contains.

ROYAL SOCIETY OF CHEMISTRY

www.rsc.org/pps

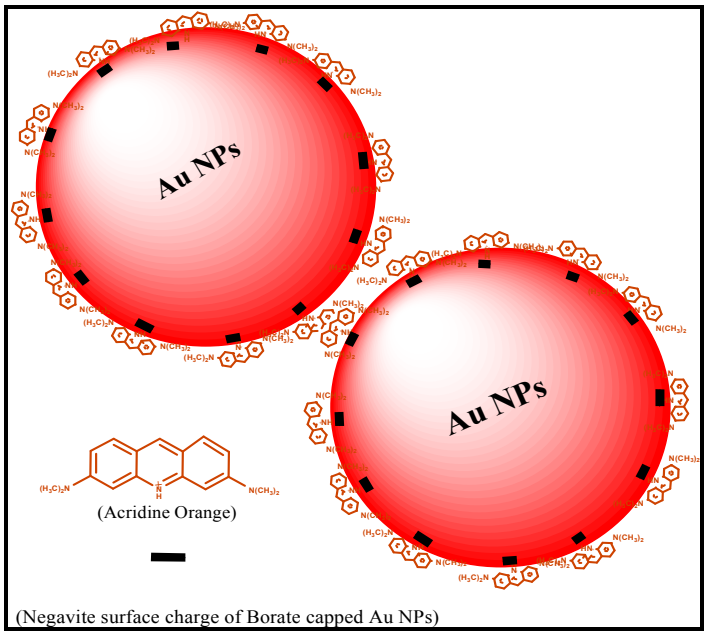

Photochemical & Photobiological Sciences Accepted Manuscript

Journal Name

RSCPublishing

ARTICLE

Elucidation of photophysical changes and orientation of acridine orange dye on the surface of borate capped gold nanoparticles by multi spectroscopic techniques

Arumugam Selva Sharma and Malaichamy Ilanchelian*

Cite this: DOI: 10.1039/x0xx00000x

Received ooth January 2012,
Accepted ooth January 2012

DOI: 10.1039/x0xx00000x

www.rsc.org/

Department of Chemistry
Bharathiar University,
Coimbatore – 641046, India.

*Corresponding author
E-mail:
selvasharma.a@gmail.com,
chelian73@yahoo.com

In the present work, we have carried out a detailed investigation on the binding interaction of Acridine orange (AO) with borate capped Gold nanoparticles (Au NPs) using absorption spectroscopy, steady state emission spectroscopy, time resolved fluorescence spectroscopy, high resolution transmission electron microscopy (HR-TEM), dynamic light scattering (DLS), zeta potential measurements, Fourier transform infra red (FT-IR) and Raman spectroscopy. The phenomena of hypochromism and the appearance of coupled localized surface plasmon resonance band (LSPR) in the absorption spectral studies of AO- Au NPs system suggested the vital role of electrostatic interaction between the AO dye and Au NPs. The results from HR-TEM and DLS measurements confirmed the formation of aggregated clusters of nanoparticles. The zeta potential studies of Au NPs and AO coated Au NPs suggested the occurrence of partial surface charge neutralization of negatively charged Au NPs by cationic AO dye. The interparticle edge to edge separation distance of adjacent Au NPs revealed the presence of AO molecules in between the nano-gap of Au NPs. Emission spectral studies of AO in the presence of increasing concentrations of Au NPs indicated the existence of static quenching mechanism. Time resolved fluorescence spectroscopic study further validates the findings of steady state emission measurements. The comparison of experimental emission quenching data with the theoretically calculated value suggested the probable layered assembly of AO on the surface of Au NPs. FT-IR and Raman spectral studies further revealed the existence of electrostatic interaction and a possible horizontal orientation of AO dye molecules on Au NPs surfaces.

Introduction

In recent years, numerous efforts have been made to investigate the photophysical and photochemical behavior of multi component nano structured assemblies consisting of metals, semiconductors and photoactive dyes.[1-6] The development of such dye-metal composites is highly useful in exploiting its optical properties for chemical and biological applications, including emission quenching of small dye molecules on gold nanoparticles (Au NPs), complementary oligo nucleotides for single stranded DNA linked metal nanoparticles or bar-coded metal nanowires and fluorescent dye-doped nanoparticles for medical diagnostics and labeling.[7-12]

Studies of dye-capped metal nanoparticles have attracted much interest in various areas of basic research,[13-20] including water-soluble monolayer-protected clusters (MPCs) functionalized with tiopronin for fluorescence quenching of fluorescein and detection of DNA binding to tiopronin/ethidium MPCs[17,18] and molecular interactions involving electron or energy transfer for fluorescence quenching as a result of the proximity of dye molecules to the metal nanoparticle surface.[13]

Excitation of localized surface plasmons on metal nanoparticles or on metal nanostructures produces a strong optical near-field or evanescent field that decays exponentially away from the metal nanoparticle surface with length scales on the order of 10 nm-200 nm. This strong optical near-field leads to the enhancement of Raman signals of nearby molecules.[21] Single molecule detection using Raman scattering has been realized using this effect when the nano-gap separation and the adsorption of target molecules is precisely adjusted.[22-29]

In addition to the Surface Enhanced Resonance Raman Spectroscopic (SERRS) technique, many promising applications of dye-nanoparticle combinations continue to emerge in recent years. The interparticle interactions and reactivities, especially in cases involving chemisorbed chromophore on the NPs surface, can leads to efficient fluorescence quenching.[20,30,31] Therefore, it is necessary to

Photochemical & Photobiological Sciences Accepted Manuscript

study the emission properties of the dye- nanoparticle assemblies to understand the interparticle molecular interactions and reactivity as it is crucial for the realization of many applications. There have been several literature reports on dye-metal nanoparticle interactions,[32-36] however, only limited information is available on the adsorption mechanism and orientation behavior of photoactive dyes with metal nanoparticles. Acridine orange (AO) is an important acridine dye that has potential applications in photodynamic therapy, clinical diagnosis and as probe molecule in model biological systems to distinguish between DNA and RNA.[37-43] On the other hand, Au NPs coupled with organic dyes are widely used for SERRS technique, biomolecular labeling and as immune probes.[13] In view of these considerations AO and Au NPs have been chosen to investigate the orientation and adsorption characteristics of AO on metal nanoparticle surfaces. In the present work, the adsorption characteristics of AO on Au NPs surfaces were systematically investigated by means of absorption spectroscopy, steady state emission spectroscopy, time resolved fluorescence spectroscopy, zeta potential measurements, HR-TEM, DLS, FT-IR and Raman spectroscopy. The influence of Au NPs on the photophysical behaviour of AO viz., absorption and emission properties has been discussed. We have also predicted the most probable orientation of AO dye molecules on the Au NPs surfaces by simple theoretical calculations and spectral studies.

Materials and methods

Chemicals. Tetrachloroauric (III) acid ($H[AuCl_4]$, 99%) and Sodium borohydride ($NaBH_4$, 99%) were purchased from Sigma-Aldrich chemicals, USA and used as received. Acridine Orange (3,6-bis-dimethyl-aminoacridine) (Figure 1) was obtained from Sd fine chemicals, India. AO was purified according to the reported procedure.[43]

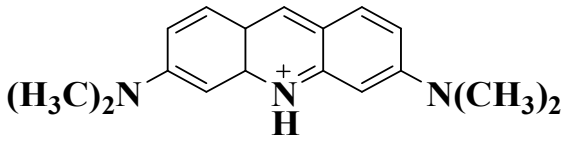

Figure 1. Structure of Acridine Orange

Preparation of borate capped gold nanoparticles. Gold nanoparticles (Au NPs) were prepared in double distilled water medium by drop wise addition of 10 ml of $H[AuCl_4]$ (6.0×10^{-4} mol dm^{-3}) into 40 ml of $NaBH_4$ (1.2×10^{-3} mol dm^{-3}) at ice cold condition with constant stirring. The molar concentration of Au NPs was calculated using the following equations (eqns. 1-2),[44]

$$N_{av} = \frac{\pi D^3}{6} \rho \left(\frac{1}{M}\right) \ldots (1)$$

$$C = \frac{N_{total}}{N_{av} V N_A} \ldots (2)$$

where, N_{av} is the average number of gold atoms per nanoparticle, D is the average diameter of the nanoparticles obtained from TEM, ρ is the density for fcc gold (19.3 g/cm^3), M is the atomic weight of gold (197 g/mol), C is the molar concentration of nanoparticle solution, N_{total} is the total number of gold atoms present in the reaction solution, V is the volume and N_A is Avogadro's number.

Molar concentration of Au NPs in the stock dispersion was computed as, Au^0_n; 2.00×10^{-8} mol dm^{-3}. The molar extinction coefficient value for the prepared nanoparticles is estimated as 2.20×10^7 dm^3 mol^{-1} cm^{-1} and it matches fairly well with the previously reported work on Au NPs.[45,46]

Spectroscopy Measurements. The concentration of AO was determined from the molar extinction coefficient (5.70×10^4 dm^3 mol^{-1} cm^{-1}) at 491 nm and the stock solution of AO was freshly prepared in double distilled water before every experiment.[47] The various concentrations of Au NPs solutions (0.40×10^{-10} mol dm^{-3} - 4.00×10^{-10} mol dm^{-3}) were prepared by pipetting an aliquot of the stock solution into a 5 ml standard measuring flask containing 1 ml of AO (4.00×10^{-6} mol dm^{-3}) and then the solutions were made up to the mark with double distilled water (pH ≈ 7). AO and Au NPs solutions were mixed uniformly and allowed to equilibrate for 15 minutes before recording the spectral data. Absorption spectral measurements were carried out using JASCO V-630 UV-visible spectrophotometer. Quartz cuvettes of path length 1 cm were used to record the absorption spectra. The emission measurements were performed on a JASCO FP-6600 spectrophotometer equipped with a xenon discharge lamp and a 1 cm quartz cell at room temperature. In emission spectral studies of AO, the excitation wavelength was set at 490 nm and the emission spectra were monitored in the wavelength range of 500 nm - 800 nm. The emission and excitation slit widths used throughout the experiments were 5 nm and 2 nm, respectively.

Time resolved fluorescence lifetime measurements were carried out by the time-correlated single-photon counting (TCSPC) method using a Horiba Jobin Yvon Fluorocube. For fluorescence lifetime measurements the samples were excited at 490 nm using a picosecond diode (IBH Nanoled-280). The emission was collected at a magic-angle polarization using a Hamamatsu micro channel plate photomultiplier (2809U). The fluorescence decays were deconvoluted using IBH DAS6 software. The goodness of fit has been assessed over the full decay including the rising edge with the help of statistical parameters χ^2 and Durbin Watson (DW).[48]

FT-IR spectral studies of AO and AO coated Au NPs in the range of 4000-400 cm^{-1} were recorded on a JASCO FT-IR-V 400 series spectrophotometer using KBr pellets. Raman spectra of AO in the absence and presence of Au NPs were recorded on R-3000-QE Raman spectrometer (Agiltron Inc, USA) equipped with a 785 nm laser excitation source. The laser beam with a laser power of 60 mW was focused onto the liquid samples kept in the Quartz cuvette.

DLS and Zeta potential measurements were performed using Zeta-sizer Nano, ZS with 633 nm He–Ne laser, equipped with a MPT-2 Autotitrator (Malvern, UK). The experimental data

Photochemical & Photobiological Sciences Accepted Manuscript

were the average of at least 20 runs. HR-TEM measurements of Au NPs in the absence and presence of AO were carried out using a JEOL JEM 2100 microscope instrument at an operating voltage of 200 kV. Samples were prepared by placing a drop of the solution onto a carbon-coated copper grid. After drying, the sample was examined by HR-TEM. The size of more than 50 particles in the TEM image was measured to obtain the average particle size.

Results and discussion

Absorption spectral studies of AO in presence of Au NPs. The reactivity of AO dye with Au NPs was characterized using absorption spectroscopy. Au NPs exhibit a strong surface plasmon band at 512 nm (see supporting information, S1).[49] The absorption spectra of AO in presence of increasing concentrations of Au NPs are shown in Figure 2. In the absence of Au NPs, AO exhibits a characteristic absorption band at 491 nm owing to the monomeric form in aqueous solution (Figure 2 (a)).[47] It can be seen from Figure 2 that with the addition of increasing concentrations of Au NPs, the absorption intensity of AO at 491 nm decreased without any significant shift in the absorption maxima with concomitant appearance of a new band in the wavelength region between 500 nm-700 nm. The two isosbestic points observed around 413 nm and 523 nm respectively, indicates the reactivity involving two species i.e. a reactant and product. The enlarged wavelength region between 500 nm and 800 nm is shown in Figure 2 (Inset). As shown in the inset of Figure 2, the absorption intensity of the new band between 600 nm and 700 nm region showed an increase with the addition of Au NPs. The absorption intensity of the new band is found to be highly dependent on the concentration of Au NPs added to the solution. It has been previously reported that the interaction of metal nanoparticles with organic molecules alters the electron density on the surface of gold nanoparticles, thereby directly affecting the surface plasmon absorption band of nanoparticles and absorption profile of the surface-bound organic moiety.[50] As a result, the decrease in absorption intensity of AO dye and the appearance of new band between 600 nm to 700 nm could be attributed to the interaction between the cationic AO dyes and negatively charged Au NPs.

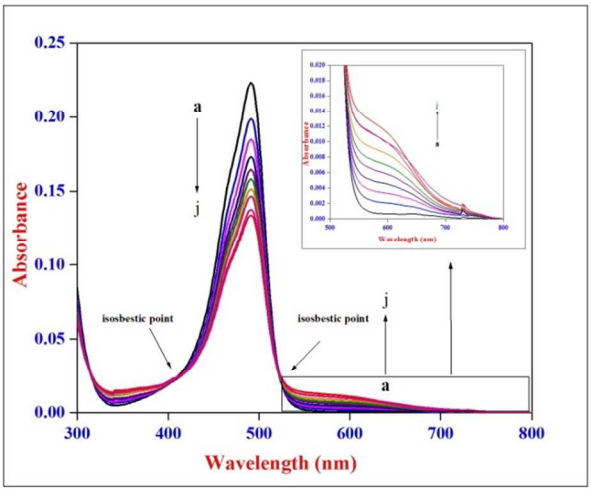

Figure 2. Absorption spectra of AO [4.00×10^{-6} mol dm^{-3}] at various Au NP concentrations. [Au NPs]: (a) 0.00, (b) 0.40×10^{-10}, (c) 0.80×10^{-10}, (d) 1.20×10^{-10}, (e) 1.60×10^{-10}, (f) 2.00×10^{-10}, (g) 2.40×10^{-10}, (h) 2.80×10^{-10}, (i) 3.20×10^{-10} and (j) 3.60×10^{-10} mol dm^{-3}. Inset shows the increase in coupled surface plasmon band of Au NPs due to aggregation.

It has been known that Au NPs, prepared by the reduction of $H[AuCl_4]$ with sodium borohydride, have a negative surface charge due to the physisorbed borate based anions. Since each borohydride anion has four reactive hydride arms, it can reduce four gold ions (+3 charge state) to neutral gold atoms and the excess borohydride anions act as stabilizing agent.[49] Accordingly in the present case, it is believed that with the addition of Au NPs to the AO solution, AO dye molecules readily gets adsorbed on the nanoparticle surface due to the electrostatic attractive force acting between the cationic AO dye molecules and the negatively charged Au NPs surface. It has been widely emphasized that the decrease in absorption intensity of dye molecules with increasing concentration of nanoparticles leads to close packing of dye molecules on a charged nanoparticle surface owing to non-covalent binding, such as electrostatic interaction.[50-57] Therefore, in the present scenario the AO- Au NPs composites could coalesce to form larger clusters due to close packing of dye molecules and charge neutralization on the nanoparticle surfaces. This in turn leads to decrease in interparticle distance of individual Au NPs and thereby result in the formation of coupled surface plasmon band (Figure 2 inset). From the above analysis, it is presumed that the phenomenon of hypochromism is associated with the crucial role of electrostatic interactions in the complexation of AO with Au NPs. Thus, the formation of new band between 600 nm to 700 nm is ascribed to the formation of aggregated clusters of AO- Au NP composites and coupling of localized surface plasmon band.[56,57]

To further ascertain the contribution of surface plasmon band of Au NPs to the observed new band in the longer wavelength region between 600 nm - 700 nm (Figure 2 inset), we have recorded the absorption spectra of Au NPs with increasing concentrations of AO (from 1.50×10^{-7} to 4.50×10^{-7} mol dm^{-3}) (Figure 3). As illustrated in Figure 3, in the absence of AO, Au

Photochemical & Photobiological Sciences Accepted Manuscript

NPs exhibit a surface plasmon band at 512 nm (Figure 3 (a)). Upon increasing the concentrations of AO to the Au NPs solution, the surface plasmon band of Au NPs was red shifted towards a longer wavelength region (562 nm) (Figure 3 (a-d)).

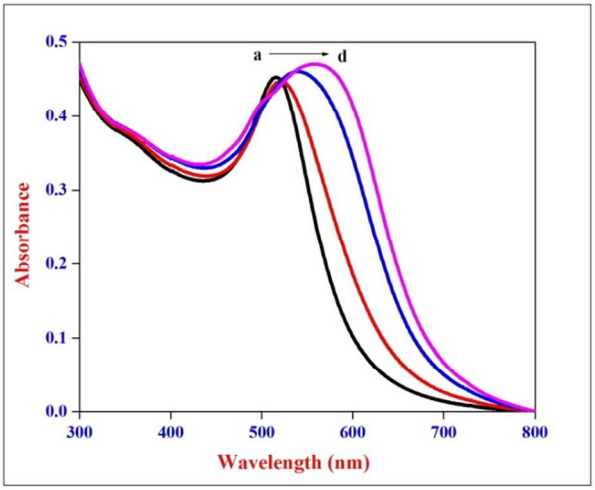

Figure 3. Absorption spectra of Au NPs [2.00 × 10^{-8} mol dm^{-3}] at various concentrations of AO. [AO]: (a) 0.00, (b) 1.50 × 10^{-7}, (c) 3.00 × $10^{-7}$and (d) 4.50 × 10^{-7} mol dm^{-3}.

In general, the position of the surface plasmon band of metal nanoparticles is very sensitive to the interparticle distance, surface adsorbed species and the surrounding dielectric medium.[50] Accordingly in the present case, the surface adsorption of AO dyes have resulted in dampening and broadening of the surface plasmon band of Au NPs with a significant red shift from 512 nm to 562 nm. As evidenced from Figure 3, the shift in surface plasmon band of Au NPs is strongly dependent on the concentration of AO dye. The observed spectral evolution and the change in colour of the solution from red to purple upon the addition of AO further reiterate the formation of larger-sized clusters of AO-Au NPs (as discussed in the previous section) (see supporting information S2).

It is well known that the magnitude of assembly induced plasmon shift depends on the strength of interparticle coupling, which in turn, depends on the proximity of the individual nanoparticles. The extent of plasmon shift thus gives a measure of the distance between the neighboring Au NPs. From the above discussion, it can be emphasized that the interparticle distance of the adjacent AO adsorbed Au NPs along with the average diameter of individual Au NPs can be utilized to gain quantitative information on the thickness of the adsorbed AO layer on the Au NPs surface. The interparticle separation between the adjacent nanoparticles can be evaluated from the following plasmon ruler equation (eqn 3),[58]

$$\frac{\Delta\lambda}{\lambda_0} \approx 0.18 \exp\frac{-(s/D)}{0.23} \ldots (3)$$

where, $\Delta\lambda/\lambda 0$ is the fractional plasmon shift, s is the interparticle edge-to-edge separation between the surface of nanoparticles, D is the particle diameter and 0.23 is the decay constant for the universal trend of $\Delta\lambda/\lambda_0$ versus s/D plot.[58]

The interparticle separation of Au NPs pair calculated using the $\Delta\lambda/\lambda_0$ plasmon shift at varying concentration of AO is listed in Table 1. As shown in Table 1, the interparticle distance between Au NPs decreased with the increase in AO dye concentrations. Similar kind of result has been reported earlier for clustered protein-coated Au NPs.[59]

Table 1. Interparticle separation distance of adjacent Au NPs in presence of AO.

Concentration of AO (mol dm^{-3})	Fractional plasmon shift $\Delta\lambda/\lambda_0$ %	Interparticle separation distance *s* (nm)
1.5 × 10^{-7}	2.10	1.4
3.0 × 10^{-7}	5.60	1.0
4.5 × 10^{-7}	10.10	0.80

The decrease in interparticle distance is associated with rapid electrostatic adsorption of AO on to the nanoparticle surface and this makes it clear that within the interparticle gap of Au NPs, layer of AO is formed with a considerable thickness. From the above interpretation, it is inferred that the existence of π–π interactions between adjacently located surface bound AO molecules could have also played a vital role in facilitating the formation of aggregated nano-clusters along with strong electrostatic interactions. Moreover, the decrease in interparticle distance between the individual AO adsorbed Au NPs substantiate the formation of coupled localized surface plasmon band. The schematic representation of electrostatic and π–π interactions for the adsorbed AO dye molecules on negatively charged Au NPs is displayed in Scheme 1.

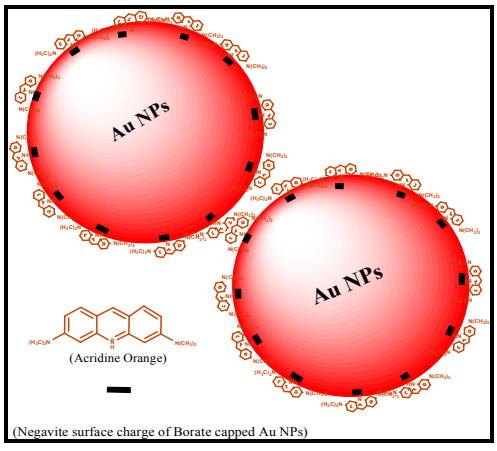

Scheme 1. Schematic illustration of electrostatic and π–π interactions for the adsorbed AO dye molecules on the negatively charged Au NPs.

Photochemical & Photobiological Sciences Accepted Manuscript

HR-TEM, DLS and Zeta potential measurements of AO-Au NPs system. The size and morphology of Au NPs in the absence and presence of AO were examined by HR-TEM measurement. Typical HR-TEM images of colloidal dispersion of Au NPs and AO adsorbed Au NPs along with the corresponding particle size distributions (Frequency %) and selective area energy dispersion (SAED) pattern are displayed in Figure 4 [A (i-iii) & B (i-iii)]. Based on HR-TEM measurements, it was found out that the Au NPs in the absence of AO are nearly spherical in shape with an average diameter of 6 nm and showed a relatively narrow size distribution [Figure 4A (i & ii)]. As depicted in Figure 4B (i), the HR-TEM image of Au NPs in the presence of AO (4.50×10^{-7} mol dm^{-3}) reveals the presence of highly clustered nanoparticles. The micrograph clearly shows that the Au NPs are glued together via AO dye adsorbed on their surfaces with an effective inter particle linkage and the size of these assemblies was found to be in the range of 13 nm. The formation of aggregated clusters of Au NPs in the presence of AO was further evidenced from the absence of free nanoparticles (Figures 4A (ii)). Recently, similar type of observations have been reported for 5, 5-disulfopropyl-3,3-dichlorothiacyanine dye on Au NPs.[60,61] As illustrated in Figures 4A (iii) and 4B (iii), the Debye–Scherrer rings in SAED patterns indicates that both Au NPs and AO adsorbed Au NPs are crystalline in nature.[62]

The particle size distribution measurements for Au NPs dispersions in the absence and presence of AO dye were performed by DLS method. The particle size distribution of Au NPs (2.00×10^{-8} mol dm^{-3}) in the absence and presence of AO (4.50×10^{-7} mol dm^{-3}) are displayed in Figure 4C (i) & 4C (ii), respectively. As shown in Figure 4C (i-ii), the addition of AO to the nanoparticle solution resulted in the increase of average particle size of Au NPs from 8±2 nm to 23±2 nm. The change in nanoparticle size clearly indicated the occurrence of AO induced aggregation of Au NPs. It is pertinent to note that the comparison of TEM and DLS measurements showed that the average particle sizes calculated from TEM were smaller than that obtained by DLS studies. This deviation in particle size measurements is ascribed to the fact that the particle size obtained by DLS measurements represents the hydrodynamic diameter of a sphere (i.e., diameter of particle with hydration shell), having the same volume as the particle and the added solvent or stabilizer moving with the particle.[60,61] It has been previously reported that DLS analysis should only be used for qualitative comparison to other characterization methods due to its low resolution and lack of robustness relative to cumulants analysis.[63] Thus, the results obtained from DLS studies were compared with absorption and TEM measurements. It was found that the outcome of DLS measurements suggested the cluster formation of Au NPs in the presence of AO and it unambiguously complement the conclusion drawn from both absorption and TEM measurements.

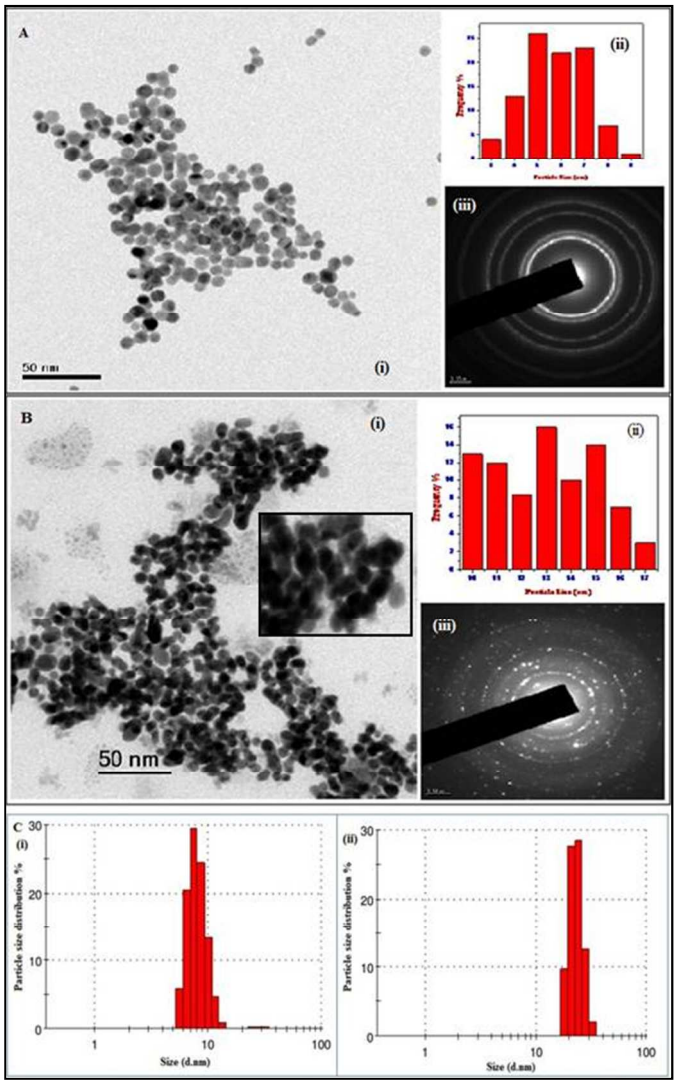

Figure 4. (A) (i) HR-TEM image of Au NPs in the absence of AO (ii) Particle size distributions (iii) SAED pattern and **(B)** (i) HR-TEM image of Au NPs in the presence of AO (Inset shows the clustered Au NPs) (ii) Particle size distributions (iii) SAED pattern. **(C)** Particle size distribution obtained from DLS measurements for Au NPs (i) in the absence and (ii) presence of AO.

Zeta potential measurements for Au NPs dispersions in the absence and presence of AO dye were carried out under the same experimental conditions as described above. In the absence of AO dye, Au NPs exhibited a zeta potential value of -47.70 mV. The negative zeta potential value suggested that the Au NPs surface is negatively charged and the electrostatic repulsion between the negative charges protects the Au NPs from aggregation. The addition of AO dye to colloidal dispersion of Au NPs induced a slight decrease of the zeta potential from -47.70 mV to -35.70 mV owing to the electrostatic interaction between negatively charged Au NPs and cationic AO dye. The observed slight decrement in zeta potential value is ascribed to the partial surface charge neutralization, which occurs due to the electrostatic adsorption of cationic AO dye molecules on the surface of Au NPs. It is well known that the surface charge neutralization involving

Photochemical & Photobiological Sciences Accepted Manuscript

electrostatic interaction of a positively charged AO dye with the negatively charged Au NPs often lead to the formation of nanoparticle aggregates.[60,61] In addition to the above observations, the conductivity measurement of Au NPs in the absence of AO showed a value of 192.00 μS cm^{-1}. However, in the presence of AO dye the conductivity of Au NPs showed a slight increase from 192.00 μS cm^{-1} to 194.00 μS cm^{-1}. Similar kind of increase in the conductivity, owing to dye aggregation on the surface of Au NPs and SnO_2 electrode had been reported earlier.[60,61,64] As a result, the slight increase in the conductivity value can be attributed to the adsorption of AO dye on the surface of Au NPs. The outcome of HR-TEM and zeta potential measurements makes it clear that the diffuse layer repulsion of negatively charged Au NPs was reduced upon the adsorption of the AO dye, thereby resulting in the formation of aggregated clusters. These observations further lend evidence to the observed hypochromism and the formation of coupled localized surface plasmon band in the absorption spectra of AO- Au NPs system (Figure 2).

Emission spectral studies of AO in presence of Au NPs. Emission spectral study is an excellent probe for revealing the electronic characteristics of dye-nanocomposites. To gain further insight into the interaction of AO dye with Au NPs, we have carried out steady state emission spectral studies. The emission spectra recorded for AO with the increasing concentrations of Au NPs are shown in Figure 5. In the absence of Au NPs, AO exhibits an emission maximum at 530 nm,[47] when excited at 490 nm (Figure 5a). As depicted in Figure 5, with the addition of increasing concentrations of Au NPs we observed a progressive decrease in the emission intensity of AO (Figure 5 (b-k)). The decrease in emission intensity indicates that a large fraction of excited AO molecules are quenched by the Au NPs.

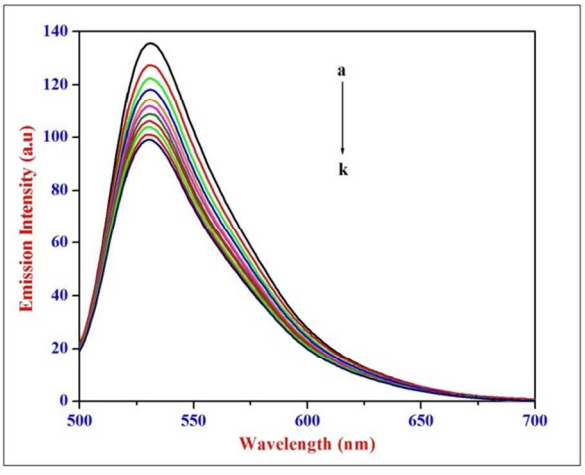

Figure 5. Emission spectra of AO [4.00 ×10^{-6} mol dm^{-3}] at various concentrations of Au NP. [Au NPs]: (a) 0.00, (b) 0.40 × 10^{-10}, (c) 0.80 × 10^{-10}, (d) 1.20 × 10^{-10}, (e) 1.60 × 10^{-10}, (f) 2.00 × 10^{-10}, (g) 2.40 × 10^{-10}, (h) 2.80 × 10^{-10}, (i) 3.20 × 10^{-10}, (j) 3.60 × 10^{-10} mol dm^{-3} and (k) 4.00 × 10^{-10} mol dm^{-3}.

It can be clearly evidenced from Figure 5 that the emission quenching of AO dye is dependent on the concentration of Au NPs added. Previous studies have shown that the emission intensity of dyes were completely quenched via attractive electrostatic interaction between dye–quencher pairs.[19,21,60,61] Therefore, the interaction of AO with Au NPs could be driven by electrostatic interaction. However, another important factor which could lead to decrease in emission intensity is the inner filter effect (IFE). The inner-filter effect refers to the absorbance of light at the excitation or emission wavelength by the compounds present in the solution. Accordingly, the influence of IFE of Au NPs on AO emission quenching has to be removed before conducting an analysis of the quenching mechanism. The correction of emission intensity can be achieved by measuring the absorbance value at the excitation and emission wavelength for each concentration of Au NPs and then multiplying the observed emission intensity value. Thus, to account for IFE the emission intensities of AO were corrected according to the equation, eqn 4: [61,65]

$$F_{Corr} = F_{Obs} \times e^{\frac{(A_{exi}+A_{emi})}{2}} \quad \ldots (4)$$

where, F_{corr} and F_{obs} is the corrected and observed emission intensities, respectively, A_{exi} and A_{emi} are the solution absorption at the excitation and emission wavelengths, respectively.

Quenching mechanism. Quenching can occur by different mechanisms namely dynamic and static quenching processes. Dynamic quenching occurs when the excited-state fluorophore is deactivated upon contact with the quencher. In static quenching process a non-fluorescent complex is formed between the fluorophore and the quencher. The exact type of quenching mechanism involved in the AO-Au NPs system (Figure 5) was evaluated with the help of Stern-Volmer equation (eqn 5),[65]

$$\frac{F_0}{F} = 1 + k_q \tau_0 [Q] = 1 + k_{SV}[Q] \ldots (5)$$

where, F_0 and F are the corrected emission intensities in the absence and presence of quencher, respectively. K_q is the bimolecular quenching constant; τ_0 is the average lifetime of the fluorophore in the absence of quencher and [Q] is the concentration of the quencher. K_{SV} is the Stern-Volmer quenching constant which measures the efficiency of quenching.

The emission quenching data of AO in the presence of Au NPs (Figure 5) were plotted as relative corrected emission intensity at maximum wavelength *vs* the concentration of Au NPs and is shown in Figure 6.

Photochemical & Photobiological Sciences Accepted Manuscript

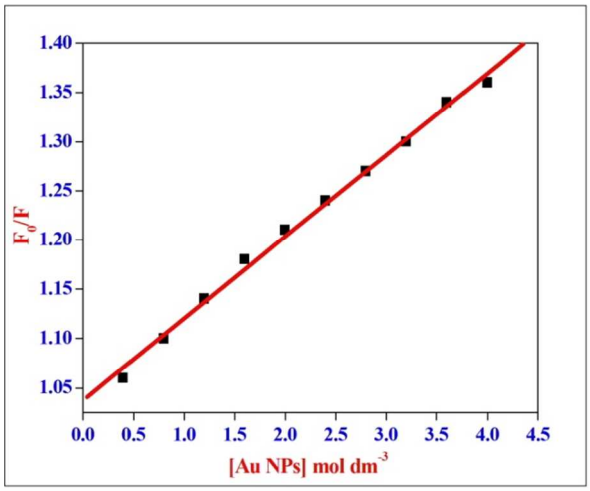

Figure 6. Stern-Volmer plot for emission quenching of AO in presence of Au NPs. (λ_{emi} = 530 nm).

It shows that within the investigated nanoparticle concentrations, the Stern-Volmer plot exhibited a good linear relationship (Figure 6). The Stern-Volmer quenching constant (K_{SV}) determined from the slope and intercept of the linear plot gives a value of 8.30×10^8 dm^3 mol^{-1} ($R^2 = 0.998$). The average lifetime (τ_0) of AO without any quencher was determined experimentally from the decay-time profile of AO and it was found as ~1.26×10^{-9}s. The obtained life time value of AO is in good conformity with an earlier report.[47] The bimolecular quenching constant K_q for the AO-Au NPs system, derived from the relation $K_q = K_{SV}/\tau_0$ is 6.58×10^{17} dm^3 mol^{-1} s^{-1}. It has been well established that for a static quenching process, the quenching constant K_q is far greater than the maximum scatter collision quenching constant (2.00×10^{10} dm^3 mol^{-1} s^{-1}).[65] The higher value of K_q for AO-Au NPs system and absorption spectral changes of AO in the presence of Au NPs (Figure 2) suggest that the quenching process is not initiated by collision, whereas, it is primarily due to complex formation viz., static quenching. It was reported that enormously high values of K_{SV}, in the case of cationic conjugated polymers and chlorophyll *a* in the presence of Au NPs is ascribed to the static quenching mechanism.[66,67] The high value of K_{SV} for the quenching of AO dye by Au NPs further substantiate the involvement of static quenching mechanism.

Time resolved fluorescence spectroscopic studies. Time-resolved fluorescence spectroscopic study has been performed to determine the origin and quenching of AO dye by Au NPs. The following expression was used to analyze the experimental time-resolved fluorescence decays P(t), eqn 6,[65]

$$P_{(t)} = b + \sum_{i}^{n} \alpha_i \exp(-t/\tau_i) \quad \ldots (6)$$

where, n is the number of discrete emissive species, b is a baseline correction, α_i and τ_i are the pre-exponential factors and excited-state fluorescence lifetimes associated with the i^{th} component, respectively. The quality of the fits and the mono- or bi-exponential nature of the decays were judged by reduced chi-square (χ^2) values and the distribution of the weighted residuals among the data channels. For all accepted fits, the χ^2 value was close to unity and the weighed residuals were distributed randomly among the data channels.[48]

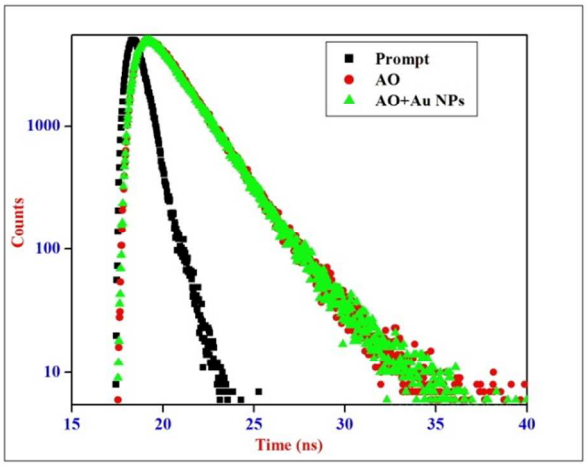

Figure 7. Time resolved fluorescence decay profile of [●] AO dye alone c[AO] = 4.00×10^{-6} mol dm^{-3} and [Δ] AO dye in the presence of Au NPs. c[Au NPs] = 4.00×10^{-10} mol dm^{-3}. (λ_{exi} = 490 nm and λ_{emi} = 530 nm).

The excited-state life time measurements of AO dye solution (4.00×10^{-6} mol dm^{-3}) in the absence and presence of Au NPs (4.00×10^{-10} mol dm^{-3}) were performed (Figure 7). It can be seen from Figure 7 that the photoluminescence decay time of the AO dye solution in the absence of Au NPs is a bi-exponential with **an average** life time value of ≈ 1.26 ns. The observed bi-exponential decay curve for AO is found to be in good agreement with the previously reported work.[68] The life time value of AO in the presence of Au NPs also exhibited a bi-exponential curve with **an average** life time value of ≈ 1.14 ns (Table 2). As shown in Figure 7 and Table 2, the time resolved fluorescence curve and decay time of AO dye in the presence of Au NPs showed no significant change from that of the free AO dye. It is well known that the formation of ground state complex between a fluorophore and metal nanoparticles cannot induce change in the excited state life times of the fluorophore.[65] Therefore, it is obvious that the unchanged fluorescence lifetime of AO in the presence of Au NPs is primarily initiated by ground state complexation of AO with Au NPs rather than by dynamic collision quenching mechanism. Furthermore, this conclusion is apparent from the absorption and steady state emission spectral studies.

Photochemical & Photobiological Sciences Accepted Manuscript

Table 2. Time resolved fluorescence decay parameters.

System	α_1	τ_1 [a] (ns)	α_2	τ_2 [a] (ns)	$\langle\tau\rangle$ [a] (ns)	χ^2
AO alone	0.91	1.00	0.08	4.03	1.26	1.09
AO in presence of Au NPs	0.95	0.99	0.04	3.99	1.14	1.14

a= ± 5% and $\langle\tau\rangle = \tau_1 \alpha_1 + \tau_2 \alpha_2$. The magnitude of χ^2 denotes the goodness of the fit.

Orientation of AO dyes on the surface of Au NPs. In the emission quenching experiment, we assumed that the quenching occurs only for those AO molecules that have direct interaction with the Au NPs surface. Depending on the orientation of the adsorbed AO, the maximum of the quenched AO dye is assumed to be restricted to full monolayer coverage on the Au NPs surface. For a single AO dye molecule approximated as a rectangular box with dimensions 0.47 nm × 1.37 nm × 0.68 nm, two possible orientations of AO dye on the nanoparticle surface can be considered namely the horizontal orientation and vertical orientation. By knowing the diameters of Au NPs (obtained from TEM measurements), the number of AO molecules needed to cover one Au NP and the number of AO moles per cm^2 adsorbed on a single Au NP can be calculated for the two possible dye orientations. It was estimated that a single Au NP (6 nm) can accommodate ≈ 121 AO dye molecules (for horizontal orientation) and ≈ 354 AO dye molecules (for vertical orientation) to form full monolayer coverage of AO dye on its surface. For an initial concentration of AO dye (4.00×10^{-6} mol dm^{-3}) consisting of 1.20×10^{16} dye molecules, the concentration of Au NPs required to form a full monolayer coverage was estimated at 1.65×10^{-10} mol dm^{-3} for horizontal orientation and 5.62×10^{-11} mol dm^{-3} for vertical orientation.

The dependence of emission intensity of AO dye with respect to increasing concentration of Au NPs is shown in Figure 8. It is evident from Figure 8 that the experimental titration end point was not reached. As suggested in an earlier report, experimental end point was determined by extrapolating the straight line to zero emission and it was found as 14.50×10^{-10} mol dm^{-3}.[61,62] The end point thus obtained is remarkable for the fact that it is larger than the calculated values of Au NPs needed to form single monolayer coverage for two different AO dye orientations, thereby suggesting possible formation of AO multilayer and the likelihood of horizontal orientation of AO on the nanoparticle surfaces. On the basis of the emission quenching end point, Chen and co workers proposed a horizontal orientation of Rhodamine B dye molecules on thioglycolic acid capped Au NPs surface.[69]

In the emission quenching experiment, it is assumed that the quenching occurs only for those AO molecules that have direct interaction with the Au NPs surface. Thus, on the basis of the loss of emission intensity observed upon Au NPs titration (4.00 × 10^{-10} mol dm^{-3}) into the AO solution, the average number of AO bound to the surface of a single Au NPs was approximately estimated as 2.70×10^3. The average number of AO molecules on the surface of Au NPs calculated from the quenching data deviates significantly from that of the theoretically calculated values for both horizontal (121 AO dye molecules) and vertical orientation (354 AO dye molecules) of AO, thereby demonstrating the probable multilayer formation or aggregation of AO on Au NPs surface. Further, the outcome of this calculation clearly suggests that binding of AO to Au NPs continues beyond the formation of an initial monolayer and that cooperative binding interaction between AO molecules may play an important role in the possible multi layer formation. Moreover, this calculation is consistent with the absorption spectral studies of Au NPs with AO. From the above theoretical calculations it is believed that the probable multilayer formation of AO dye molecules on Au NPs can be attained only if the AO molecules are oriented towards the nanoparticle surface in a horizontal orientation.

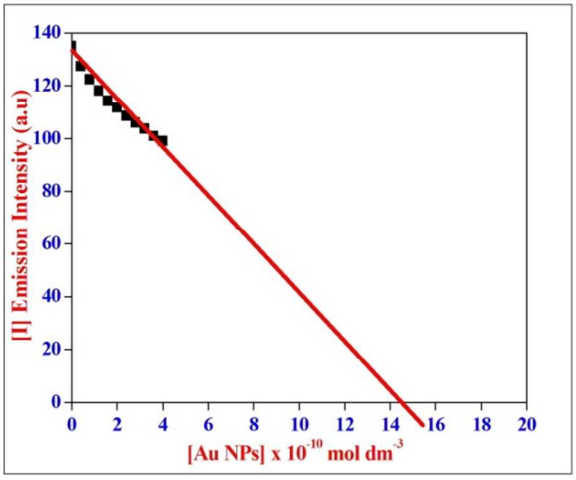

Figure 8. Plot of the Emission intensity at 530 nm *vs* the concentration of bare Au NPs.

FT-IR and Raman Spectral studies of AO-Au NP system. The adsorption mechanism of AO on Au NPs surfaces was further characterized by FT-IR and Raman spectroscopy. The FT-IR spectra of free AO and AO coated Au NPs are shown in Figure 9 (A&B). The FT-IR spectrum of free AO shows a band around 1594 cm^{-1} characteristic of skeletal vibration of the phenyl ring of AO and the band around 3438 cm^{-1} is ascribed to the N-H stretching vibration (Figure 9A). In the FT-IR spectrum of AO coated Au NPs (Figure 9B) the band corresponding to skeletal vibration of the phenyl ring was also observed around 1592 cm^{-1} (Figure 9B). This confirms the presence of AO on the surface of Au NPs whereas, the N-H stretching vibration of AO coated Au NPs is shifted towards a lower frequency of around 3211 cm^{-1} (Figure 9B). Similar type of FT-IR spectrum has been reported for thionine dye adsorbed on the surface of citrate capped Au NPs.[70] In the present case, it is believed that the observed shift in N-H vibrational frequency of AO adsorbed on

Photochemical & Photobiological Sciences Accepted Manuscript

Au NPs is attributed to the interaction between positively charged NH+ moiety of the central phenyl ring of AO with the negatively charged boron based Au NPs.[71,72] Based on the relative enhancement in the SERR spectra of AO coated silver colloids and silver island films, Zimmermann and co workers concluded that AO dye adsorbs onto the surface of silver nanoparticles in a slightly slanted orientation in such a way that the adsorption geometry lie in between both horizontal and vertical orientation.[73,74] However, our findings are contrary to the previously reported work[73] and this deviation could be accounted well on the fact that the formation of layered assemblies of AO molecules on silver colloids was not considered in the previous report. Moreover, it is difficult to conclude the probable orientation of AO on the nanoparticle surface solely on the basis of SERR alone, as the cationic AO induces aggregation of nanoparticles. The surface contribution of metal colloids to the SERR spectrum of AO could arise from clustered nanoparticles as well. The formation of clustered gold nanoparticles in the presence of cationic AO dye and the ability of AO dye to form a parallel array in stacked configuration have also been reported.[2,74] Thus, in the present case the outcome of the emission and FT-IR spectral studies clearly indicated the possibility of layered assemblies of AO on the nanoparticle surface in a horizontal orientation. Further, the occurrence of electrostatic interaction between the NH^+ moiety in the central phenyl ring of AO dye and the negatively charged Au NPs can be possible only if the AO molecules are oriented in a horizontal orientation. Thus, on the basis of experimental and theoretical results, the adsorption of AO on the Au NPs is considered to involve electrostatic interaction in a horizontal orientation.

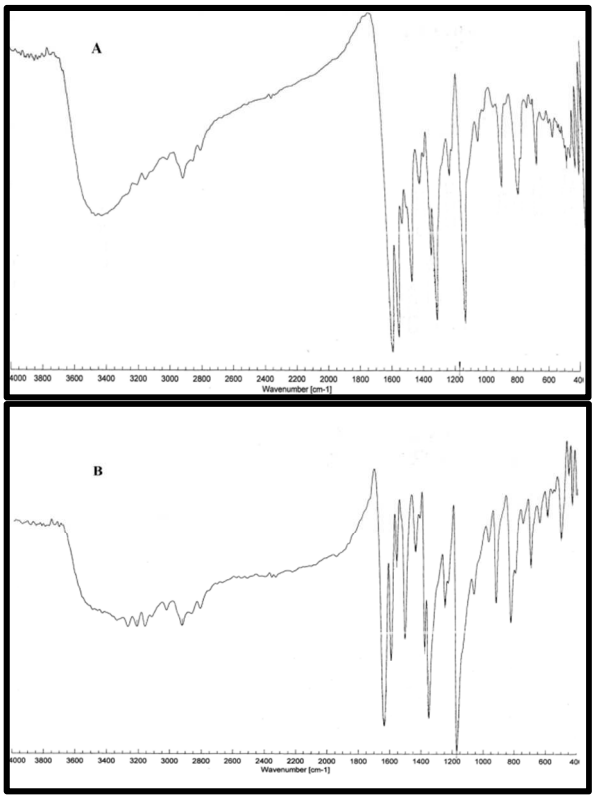

Figure 9. FT-IR spectra of **(A)** AO alone and **(B)** AO adsorbed on the surface of Au NPs.

The Raman spectral measurements of AO dye solution (4.00×10^{-6} mol dm^{-3}) in the absence and presence of Au NPs (4.00×10^{-10} mol dm^{-3}) were performed (Figure 10 (a-b)). As shown in Figure 10 (a), the Raman frequencies pertaining to AO matches fairly well with the previously reported literature work.[75] For example the peak frequencies around 1541 cm^{-1} (very weak) and 1398 cm^{-1} (very weak) is due to the presence of ring and CN stretching vibrations, respectively. The band around 1347 cm^{-1} (strong) is attributed to the overlapping signals of CH_3 and C=N stretching modes. The signal around 1214 cm^{-1} (weak band) mainly arises due to the ring deformation modes, C=C and C=N bonds. Most of the medium bands in the region between 700-400 cm^{-1} were assigned to out of plane ring and CH deformational modes. As depicted in Figure 10 b, the peak frequencies in the Raman spectrum of AO coated Au NPs was similar to AO spectra. The identical vibrational frequencies in the Raman spectra of both AO and AO coated Au NPs enabled us to conclude that the AO dye is adsorbed on the surface of Au NPs. The obvious decrement in Raman peak intensities of AO coated Au NPs also suggested the existence of interaction between AO and Au NPs. Recently, the identification of thiacyanine dye aggregates on the Au NPs surface by comparing the spectra of dye nano-conjugates and the known Raman spectra of aggregated thiacyanine dyes have also been reported.[63] Thus, on the basis of Raman spectral studies it is concluded that AO dye is strongly bound to the Au NPs and it complements the findings of FT-IR results.

Photochemical & Photobiological Sciences Accepted Manuscript

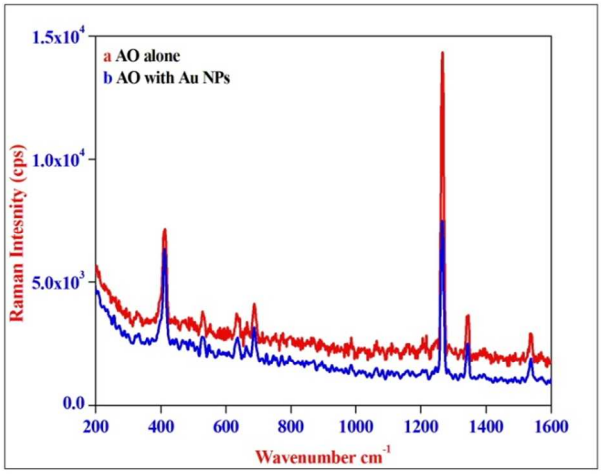

Figure 10. Raman spectra of AO [4.00 × 10^{-6} mol dm^{-3}] in the presence of Au NPs (a) 0.0 and (b) 4.00×10^{-10} mol dm^{-3}.

Conclusions

In conclusion, the results described herein provide deep insight into the adsorption characteristics of AO dye on the surface of Au NPs surface. Addition of increasing concentrations of Au NPs to AO dye solution brought about significant changes in the absorption spectra of AO dye. The observed spectral changes of AO are primarily attributed to the electrostatic interaction of cationic AO dye with the negatively charged Au NPs. The results from HR-TEM, DLS and zeta potential measurements of AO-Au NPs system confirmed the formation of cluster assemblies and a partial surface charge neutralization of negatively charged Au NPs by cationic AO dye. The steady state emission measurements of AO-Au NPs system clearly indicated the emission quenching properties of Au NPs. The emission quenching of AO dye in presence of increasing concentrations of Au NPs substantiate the findings of absorption titration experiments and it was found that the quenching mechanism follows a static quenching process. Time resolved fluorescence spectroscopic measurements of AO in the presence of Au NPs confirmed the origin and mechanism of quenching process as static quenching. The possible formation of AO multilayer on the surface of Au NPs is established by comparing the experimental emission quenching data with the theoretically calculated value. The results from FT-IR study also indicated that the NH^{+} moiety of central phenyl ring of AO most probably binds to the Au NP surfaces through electrostatic interaction in a horizontal orientation. Moreover, the observations from Raman spectral data corroborate our conclusion that AO is strongly adsorbed to the surface of Au NPs. The outcome of the present investigation will serve as a precedent in understanding the photophysical and orientation behaviour of structurally similar planar dyes on metal nanoparticles. Further this study will contribute to wide range of applications in nano electronics, biosensor and biological imaging.

Electronic Supplementary Information. The absorption spectrum of Au NPs and photograph of Au NPs in presence of increasing concentrations of AO are given in supporting information.

Acknowledgements

The authors' gratefully acknowledges Department of Science and Technology (DST-SERC-FAST Track scheme. Project No.SR/FT/CS-015/2009) and University grants commission (UGC-MRP, Project No. 41-309/2012 (SR)), India for the financial support. We are thankful to Dr. S. Kabilan, Professor of Chemistry, Annamalai University for his help in carrying out the Time resolved fluorescence spectroscopic analysis.

Notes and references

1. C. Nirmala, P.V. Kamat, J. Hu and G. Jones II, Dye-Capped Gold Nanoclusters: Photoinduced Morphological Changes in Gold/Rhodamine 6G Nanoassemblies. *J. Phys. Chem. B,* 2000, **104**, 11103-11109.
2. H. Kitching, A. Kenyon and I.P. Parkin, The interaction of gold and silver nanoparticles with a range of anionic and cationic dyes, *Phys. Chem. Chem. Phys.*, 2014, **16**, 6050-6059.
3. A. Yoshida and N. Kometani, Effect of the Interaction between Molecular Exciton and Localized Surface Plasmon on the Spectroscopic Properties of Silver Nanoparticles Coated with Cyanine Dye J-Aggregates, *J. Phys. Chem. C*, 2010, **114**, 2867-2872.
4. Y. Fu, J. Zhang and J.R. Lakowicz, Metallic-Nanostructure-Enhanced Fluorescence of Single Flavin Cofactor and Single Flavoenzyme Molecules, *J. Am. Chem. Soc.* 2010, **132**, 5540-5541.
5. N. Narband, M. Uppal, C.W. Dunnill, G. Hyett, M. Wilson and I.P. Parkin, The interaction between gold nanoparticles and cationic and anionic dyes: enhanced UV-visible absorption, *Phys. Chem. Chem. Phys.*, 2009, **11**, 10513-10518.
6. K. Adachi, T. Mita, T. Yamate, S. Yamazaki, H. Takechi and H. Watara, Controllable adsorption and ideal H-aggregation behaviors of phenothiazine dyes on the tungsten oxide nanocolloid surface, *Langmuir*, 2010, **26 (1)**,117-125.
7. T. Huang and R.W. Murray, Quenching of [Ru(bpy)3]2+ Fluorescence by Binding to Au Nanoparticles, *Langmuir*, 2002, **18**, 7077-7081.
8. S.K. Ghosh, A. Pal, S. Kundu, S. Nath and T. Pal, Fluorescence quenching of 1-methylaminopyrene near gold nanoparticles: size regime dependence of the small metallic particles, *Chem. Phys. Lett.* 2004, **395**, 366-372.
9. H. Li and L.J. Rothberg, Label-Free Colorimetric Detection of Specific Sequences in Genomic DNA Amplified by the Polymerase Chain Reaction, *J. Am. Chem. Soc.* 2004, **126**, 10958-10961.
10. H.H. Li and L. Rothberg, DNA Sequence Detection Using Selective Fluorescence Quenching of Tagged Oligonucleotide Probes by Gold Nanoparticles, *J. Anal. Chem.* 2004, **76**, 5414-5417.
11. D.J. Maxwell, J.R. Taylor and S. Nie, Self-Assembled Nanoparticle Probes for Recognition and Detection of Biomolecules, *J. Am. Chem. Soc.* 2002, **124**, 9606-9612.

Photochemical & Photobiological Sciences Accepted Manuscript

12. W. Lian, S.A. Litherland, H. Badrane, W. Tan, D. Wu, H.V. Baker, P.A. Gulig, D.V. Lim and S. Jin, Ultrasensitive detection of biomolecules with fluorescent dye-doped nanoparticles, *Anal. Biochem.* 2004, **334**, 135-144.
13. K.G. Thomas and P.V. Kamat, Chromophore-Functionalized Gold Nanoparticles, *Acc. Chem. Res.* 2003, **36**, 888-898.
14. S.K. Ghosh, A. Pal, S. Nath, S. Kundu, S. Panigrahi and T. Pal, Dimerization of eosin on nanostructured gold surfaces: Size regime dependence of the small metallic particles, *Chem. Phys. Lett*. 2005, **412**, 5-11.
15. O.V. Makarova, A.E. Ostafin, H. Miyoshi, J.R. Norris and D. Meisel, Adsorption and Encapsulation of Fluorescent Probes in Nanoparticles, *J. Phys. Chem. B* 1999, **103**, 9080-9084.
16. W. Ni, H. Chen, J. Su, Z. Sun, J. Wang and H. Wu, Effects of Dyes, Gold Nanocrystals, pH, and Metal Ions on Plasmonic and Molecular Resonance Coupling, *J. Am. Chem. Soc.* 2010, **132**, 4806-4814.
17. G.L. Wang, J. Zhang and R.W. Murray, DNA Binding of an Ethidium Intercalator Attached to a Monolayer-Protected Gold Cluster, *Anal. Chem.* 2002, **74**, 4320-4327.
18. A.C. Templeton, D.E. Cliffel and R.W. Murray, Redox and Fluorophore Functionalization of Water-Soluble, Tiopronin-Protected Gold Clusters, *J. Am. Chem. Soc.* 1999, **121**, 7081-7089.
19. E. Dulkeith, M. Ringler, T.A. Klar, J. Feldmann, A. Munoz Javier and W.J. Parak, Gold Nanoparticles Quench Fluorescence by Phase Induced Radiative Rate Suppression, *Nano Lett.* 2005, **5**, 585-589.
20. I.I.S. Lim, F. Goroleski, D. Mott, N. Kariuki, W. Ip, J. Luo and C.J. Zhong, Adsorption of Cyanine Dyes on Gold Nanoparticles and Formation of J-Aggregates in the Nanoparticle Assembly, *J. Phys. Chem. B,* 2006, **110**, 6673-6682.
21. S. Murphy, L. Huang and P.V. Kamat, Charge-Transfer Complexation and Excited-State Interactions in Porphyrin-Silver Nanoparticle Hybrid Structures, *J. Phys. Chem. C,* 2011, **115**, 22761-22769.
22. X.M. Qian, X.H. Peng, D.O Ansari, Q. Yin-Goen, G.Z. Chen, D.M. Shin, L. Yang, A.N. Young, M.D. Wang and S.M. Nie, In vivo tumor targeting and spectroscopic detection with surface-enhanced Raman nanoparticle tags, *Nat. Biotechnol.* 2008, **26**, 83-.
23. E.C. Le Ru and P.G. Etchegoin, Principles of Surface Enhanced Raman Spectroscopy. Elsevier, **2009**.
24. X.-M. Qian and S.M. Nie, Single-molecule and single-nanoparticle SERS: from fundamental mechanisms to biomedical applications, *Chem. Soc. Rev.* 2008, **37**, 912-920.
25. J. Jiang, K. Bosnick, M. Maillard and L. Brus, Single Molecule Raman Spectroscopy at the Junctions of Large Ag Nanocrystals, *J. Phys. Chem. B***,** 2003, **107**, 9964-9972.
26. Z. Liu, G. Liu, H. Zhou, X. Liu, K. Huang, Y. Chen and G. Fu, Near-unity transparency of a continuous metal film via cooperative effects of double plasmonic arrays, *Nanotechnology,* 2013, **24**, 155203-1-8.
27. Z. Liu, H. Shao, G. Liu, X. Liu, H. Zhou, Y. Hu, X. Zhang, Z. Cai and G. Gu, $\lambda^3/20000$ plasmonic nanocavities with multispectral ultra-narrowband absorption for high-quality sensing, *Appl. Phys. Lett.* 2014, **104**, 081116-1-4.
28. G. Liu, Y. Hu, Z. Liu, Y. Chen, Z. Cai, X. Zhang and K. Huang, Robust multispectral transparency in continuous metal film structures via multiple near-field plasmon coupling by a finite-difference time-domain method, *Phys. Chem. Chem. Phys.,* 2014, **16**, 4320-4328.
29. T. Yajima, Y. Yu and M. Futamata, Flocculation and SERS Activation of Au Nanoparticles Using Cationic and Neutral Cresyl Violet Molecules, *e-J. Surf. Sci. Nanotech*. 2012, **10**, 417-425.
30. N. Nerambourg, M.H. Werts, M. Charlot and M.B. Desce**,** Quenching of Molecular Fluorescence on the Surface of Monolayer-Protected Gold Nanoparticles Investigated Using Place Exchange Equilibria, *Langmuir*, 2007, **23**, 5563-5570.
31. E. Dulkeith, M. Ringler, T.A. Klar, J. Feldmann, A. Munoz Javier and W.J. Parak, Gold Nanoparticles Quench Fluorescence by Phase Induced Radiative Rate Suppression, *Nano Lett.,* 2005, **5**, 585-589.
32. S. Franzen, J.C.W. Folmer, W.R. Glomm and R. O'Neal, Optical Properties of Dye Molecules Adsorbed on Single Gold and Silver Nanoparticles, *J. Phys. Chem. A*, 2002, **106**, 6533-6540.
33. J. Zhang and J.R. Lakowicz, Enhanced Luminescence of Phenyl-phenanthridine Dye on Aggregated Small Silver Nanoparticles, *J. Phys. Chem. B,* 2005, **119**, 8701-8706.
34. P.C. Lee and D. Meisel, Adsorption and Surface-Enhanced Raman of Dyes on Silver and Gold Sols, *J. Phys. Chem.,* 1982, **86**, 3391-3395.
35. S.K. Ghosh and T. Pal, Photophysical aspects of molecular probes near nanostructured gold surfaces, *Phys.Chem.Chem.Phys.,* 2009, **11**, 3831-3844.
36. A. Vujačić, V. Vasić, M. Dramićanin, S.P. Sovilj, N. Bibić, J. Hranisavljević and G.P. Wiederrecht, Kinetics of J-Aggregate Formation on the Surface of Au Nanoparticle Colloids, *J. Phys. Chem. C,* 2012, **116**, 4655-4661.
37. H. Schmidt, A. Al-Ibrahim, U. Dietzel and L. Bieker, On the acridine and thiazine dye sensitized photodynamic inactivation of lysozyme-singlet oxygen self-quenching by the sensitizers, *Photochem. Photobiol.,* 1981, **33**, 127-130.
38. F. Traganos, Z. Darzynkiewicz, T. Sharpless and M.R. Melamed, Simultaneous staining of ribonucleic and deoxyribonucleic acids in unfixed cells using acridine orange in a flow cytofluorometric system, J. *Histochem. Cytochem.,* 1977, **25**, 46-56.
39. A.K. Shaw and S.K. Pal, Fluorescence Relaxation Dynamics of Acridine Orange in Nanosized Micellar Systems and DNA, *J. Phys. Chem. B,* 2007,**111**, 4189-4199.
40. M.B. Lyles and I.L. Cameron, Interactions of the DNA intercalator acridine orange, with itself, with caffeine, and with double stranded DNA, *Biophys. Chem.* 2002, **96**, 53-76.
41. A.I. Kononov, E.B. Moroshkina, N.V. Tkachenko and H. Lemmetyinen, Photophysical Processes in the Complexes of DNA with Ethidium Bromide and Acridine Orange: A Femtosecond Study, *J. Phys Chem. B* 2001,**105**, 535-541.
42. A.C. Bhasikuttan, J. Mohanty, W.M. Nau and H. Pal, Efficient fluorescence enhancement and cooperative binding of an organic dye in a supra-biomolecular host-protein assembly, *Angew. Chem., Int. Ed.,* 2007, **46**, 4120-4122.
43. M. Yitagliano, L. Costantino and A. Zagari, Interaction between Acridine Orange and poly (styrenesulfonic acid), *J. Phys. Chem,* 1973*,* **77**, 204-210.
44. N. Nishida, E.S. Shibu, H. Yao, T. Oonishi, K. Kimura and T. Pradeep, Fluorescent Gold Nanoparticle Superlattices, *Adv. Mater.,* 2008, **20**, 4719-4723.
45. X. Liu, M. Atwater, J. Wang and Q. Huo, Extinction coefficient of gold nanoparticles with different sizes and different capping ligands, *Colloids Surf., B*, 2007, **58**, 3-7.

Photochemical & Photobiological Sciences Accepted Manuscript

46. M.M. Maye, L. Han, N.N. Kariuki, N.K. Ly, W.-B. Chan, J. Luo, V.W. Jones and C.J. Zhong, Gold and alloy nanoparticles in solution and thin film assembly: spectrophotometric determination of molar absorptivity, *Anal. Chim. Acta*, 2003, **496**, 17-27.
47. M. Shaikh, J. Mohanty, P.K. Singh, W.M. Naub and H. Pal, Complexation of acridine orange by cucurbit[7]uril and β-cyclodextrin: photophysical effects and pKa shifts, *Photochem. Photobiol. Sci.,* 2008, **7**, 408-414.
48. G. Mandal, M. Bardhan and T. Ganguly, Occurrence of Förster Resonance Energy Transfer between Quantum Dots and Gold Nanoparticles in the Presence of a Biomolecule, *J. Phys. Chem. C*, 2011, **115**, 20840-20848.
49. M.N. Martin, I.B. James, C. Paul and K.E. Sang, Charged Gold Nanoparticles in Non-Polar Solvents: 10-min Synthesis and 2D Self-Assembly, *Langmuir*, 2010, **26**, 7410-7417.
50. P.V. Kamat, Photophysical, photochemical and photocatalytic aspects of metal nanoparticles, *J. Phys. Chem. B*, 2002, **106**, 7729-7744.
51. T. Yajima, Y. Yu and M. Futamata, Closely adjacent gold nanoparticles linked by chemisorption of neutral rhodamine 123 molecules providing enormous SERS intensity, *Phys. Chem. Chem. Phys.,* 2011, **13**, 12454-12462.
52. D. Liu and P.V. Kamat, Electrochemically active nanocrystalline SnO_2 films: surface modification with thiazine and oxazine dye aggregates, *J. Electrochem. Soc,* 1995, **142**, 835-839.
53. C. Nasr, D. Liu, S. Hotchandani and P.V. Kamat, Dye-Capped Semi conductor Nanoclusters. Excited State and Photosensitization Aspects of Rhodamine 6G H-Aggregates Bound to SiO_2 and SnO_2 Colloids, *J. Phys. Chem.,* 1996, **100**, 11054-11061.
54. J. Hranisavljevic, M.N. Dimitrijevic, G.A. Wurtz, G.P. Wiederrecht, Photoinduced Charge Separation Reactions of J-Aggregates Coated on Silver Nanoparticles, *J. Am. Chem. Soc.,* 2002, **124**, 4536-4537.
55. J. Zhao, L. Jensen, J. Sung, S. Zou, G.C. Schatz and R.P. Van Duyne, Interaction of Plasmon and Molecular Resonances for Rhodamine 6G Adsorbed on Silver Nanoparticles, *J. Am. Chem. Soc.,* 2007, **129**, 7647-7656.
56. M. Futamata, T. Yanatori, T. Kokubun and Y. Yu, Closely Adjacent Ag Nanoparticles Formed by Cationic Dyes in Solution Generating Enormous SERS Enhancement, *J. Phys. Chem. C,* 2010, **114**, 7502-7508.
57. M. Futamata, Y. Yu and T. Yajima, Elucidation of Electrostatic Interaction between Cationic Dyes and Ag Nanoparticles Generating Enormous SERS Enhancement in Aqueous Solution, *J. Phys. Chem. C,* 2011, **115**, 5271-5279.
58. P.K. Jain, W. Huang and M.A. El-Sayed, On the universal scaling behavior of the distance decay of plasmon coupling in metal nanoparticle pairs: A plasmon ruler equation, *Nano Lett.*, 2007, **7**, 2080-2088.
59. S.H. De Paoli Lacerda, J.J. Park, C. Meuse, D. Pristinski, M. L. Becker, A. Karim and J. F. Douglas, Interaction of gold nanoparticles with common human blood proteins, *ACS Nano,* 2010, **4**, 365-379.
60. A. Vujacic, V. Vodnik, S.P. Sovilj, M. Dramićanin, N. Bibić, S. Milonjić and V. Vasić, Adsorption and Fluorescence Quenching of 5,5′-disulfopropyl-3,3′-dichlorothiacyanine Dye on Gold Nanoparticles, *New J. Che,* 2013, **37**, 743-751.
61. A. Vujacic, V. Vasic, M. Dramicanin, S. P. Sovilj, N. Bibic, S. Milonjic and V. Vodnik, Fluorescence Quenching of 5,5′-Disulfopropyl-3,3′-dichlorothiacyanine Dye Adsorbed on Gold Nanoparticles, *J. Phys. Chem. C,* 2013, **117**, 6567-6577.
62. N. Vasimalai and S.A. John, Aggregation and de-aggregation of gold nanoparticles induced by polyionic drugs: spectrofluorimetric determination of picogram amounts of protamine and heparin drugs in the presence of 1000-fold concentration of major interferences, *J. Mater. Chem. B,* 2013, **1**, 5620-5627.
63. D.H. Tsai, F.W. DelRio, A.M. Keene, K.M. Tyner, R.I. MacCuspie, T.J. Cho, M.R. Zachariah, and V.A. Hackley, Adsorption and Conformation of Serum Albumin Protein on Gold Nanoparticles Investigated Using Dimensional Measurements and in Situ Spectroscopic Methods, Langmuir, 2011, **27**, 2464-2477.
64. K. Iriyama, F. Mizutani and M. Yoshiura, Enhancement of photocurrent at a merocyanine-coated electrode due to chromophore aggregation, *Chem. Lett.,* 1980, **9**, 1399-1402.
65. J.R. Lakowicz, Principles of Fluorescence Spectroscopy, 3rd edition, Springer, **2006**.
66. S. Barazzouk, P.V. Kamat and S. Hotchandani, Photoinduced electron transfer between chlorophyll a and gold nanoparticles, *J. Phys. Chem. B*, 2005, **109**, 716-723.
67. C. Fan, S. Wang, J.W. Hong, G.C. Bazan, K.W. Plaxco and A.J. Heeger, Beyond super quenching: Hyper-efficient energy transfer from conjugated polymers to gold nanoparticles, *PNAS,* 2003, **100**, 6297-6301.
68. R.D Falcone, N.M. Correa, M.A. Biasutti, and J.J. Silber, Acid-Base and Aggregation Processes of Acridine Orange Base in *n*-Heptane/AOT/Water Reverse Micelles, Langmuir, 2002, **18**, 2039-2047.
69. A.F. Zheng, J. Chen, G. Wu, H. Wei, C. He, X. Kai, G. Wu and Y. Chen, Optimization of a sensitive method for the "switch-on" determination of mercury(II) in waters using Rhodamine B capped gold nanoparticles as a fluorescence sensor, *Microchim Acta.,* 2009, **164**, 17-27.
70. Y. Ding, X. Zhang, X. Liu and R. Guo, Adsorption Characteristics of Thionine on Gold Nanoparticles, *Langmuir*, 2006, **22**, 2292-2298.
71. J.A. Dean, Langes Handbook of Chemistry, McGraw-Hill, 1985.
72. K.G. Thomas and P.V. Kamat, Making Gold Nanoparticles Glow: Enhanced Emission from a Surface-Bound Fluoroprobe, *J. Am. Chem. Soc,* 2000, **122**, 2655-2656.
73. F. Zimmerman, B. Hossenfelder, J.C. Panitz and A. Wokaun, SERRS study of acridine orange and its binding to DNA strands, *J. Phys. Chem. C*, 1994**, 48**, 12796-12804.
74. D.J. Blears and S.S. Danyluk, A Nuclear Magnetic Resonance Investigation of the Aggregation of Acridine Orange in Aqueous Solution, *J. Am. Chem. Soc,* 1967, **89 (1)**, 21-26.

Photochemical & Photobiological Sciences Accepted Manuscript